Atmos. Meas. Tech. Discuss., 8, 4817–4858, 2015
www.atmos-meas-tech-discuss.net/8/4817/2015/
doi:10.5194/amtd-8-4817-2015

Atmospheric Measurement Techniques Discussions
Open Access

Global validation of improved SCIAMACHY scientific ozone limb data using ozonesonde measurements

J. Jia, A. Rozanov, A. Ladstätter-Weißenmayer, and J. P. Burrows

Institute of Environmental Physics, Bremen, Germany

Received: 13 March 2015 – Accepted: 10 April 2015 – Published: 13 May 2015

Correspondence to: J. Jia (jia@iup.physik.uni-bremen.de)

Published by Copernicus Publications on behalf of the European Geosciences Union.

Global validation of improved SCIAMACHY scientific ozone limb data

J. Jia et al.

Abstract

In this manuscript, the latest SCIAMACHY limb ozone scientific vertical profiles, namely the current V2.9 and the upcoming V3.0, are extensively compared with ozone sonde data from the WOUDC database. The comparisons are made on a global scale from 2003 to 2011, involving 61 sonde stations. The retrieval processors used to generate V2.9 and V3.0 data sets are briefly introduced. The comparisons are discussed in terms of vertical profiles and stratospheric partial columns. Our results indicate that the V2.9 ozone profile data between 20–30 km is in good agreement with ground based measurements with less than 5 % relative differences in the latitude range of 90° S–40° N (with exception of the tropical Pacific region where an overestimation of more than 10 % is observed), which corresponds to less than 5 DU partial column differences. In the tropics the differences are within 3 %. However, this data set shows a significant underestimation northwards of 40° N (up to ~ 15 %). The newly developed V3.0 data set reduces this bias to below 10 % while maintaining a good agreement southwards of 40° N with slightly increased relative differences of up to 5 % in the tropics.

1 Introduction

Stratospheric ozone is one of the most important trace gases in the atmosphere. It is well known as an absorber of UV radiation, thereby protecting the biosphere damaging from short wave electromagnetic radiation and simultaneously plays a key role in determining the temperature structure of the atmosphere (Read, 1988). Retrieving stratospheric ozone profiles with a high accuracy is not only important for stratospheric ozone studies, but also a requirement for the establishment of a long-term essential climate variable (ECV) data record. To achieve this goal, ground-based, balloon borne, airborne and satellite instruments have been used to monitor ozone abundances in the atmosphere during the last decades. For satellite instruments, different observation techniques including solar/stellar occultation measurements, e.g. SAGE, HALOE, ACE, GOMOS, limb scatter/emission measurements, e.g. MLS, MIPAS, OSIRIS and nadir measurements, e.g. GOME/GOME2, OMI, IASI, are used (see e.g. Sofieva et al., 2013; Hassler et al., 2014 and references therein). The passive imaging spectrometer SCIAMACHY (SCanning Imaging Absorption spectroMeter for Atmospheric CartograpHY) used in this study provided vertical distributions of atmospheric trace gases by employing the limb scattering measurement technique (Burrows et al., 1995; Bovensmann et al., 1999).

In this manuscript we discuss the vertical ozone profiles retrieved from SCIAMACHY limb measurements at IUP Bremen (Institute of Environmental Physics, University of Bremen, Germany). The error budget typical for a recent retrieval version was reported by Rahpoe et al. (2013). Previous validation activities done by Mieruch et al. (2012) with respect to other satellite instruments showed an agreement to better than 10 % and often within 5 % between 20 and 50 km, with a high bias below 20 km explained by a presence of high convective clouds. Tegtmeier et al. (2013) performed an intercomparison of vertically resolved monthly zonal mean ozone climatologies from 18 limb-viewing satellite instruments operated between 1978–2010, including SCIAMACHY observations. The agreement was quite good in the middle stratosphere, with maximum differences of up to +5 %. The climatologies derived from SCIAMACHY were found to show a positive bias of up to +10 % in the tropical and mid latitude upper stratosphere (5–1 hPa).

The current SCIAMACHY data set distributed by IUP Bremen is V2.9. Previous comparisons of this data set to ozone sondes showed a severe underestimation of the ozone concentration in the northern high latitudes with a systematic bias of up to ~ 15 % between 15 and 30 km. The reason for that is believed to be the instrumental stray light occurring at small relative azimuth angles (sun is close to the instrument field of view) typical for the measurements at high northern latitudes. Because at these angles, for a 10:00 a.m. equator crossing time instrument in descending node, the scattering of extra terrestrial solar radiation from the platform could most likely baffles into the instrument field of view which influences the measurement results. To eliminate

AMTD
8, 4817–4858, 2015

Global validation of improved SCIAMACHY scientific ozone limb data

J. Jia et al.

the observed negative bias, a new version of SCIAMACHY ozone limb data, V3.0, has been developed. As demonstrated by the validation with ozone sondes, significant improvements have been achieved.

Here, we present validation results comprising 10 years SCIAMACHY limb data of versions V2.9 and V3.0 using globally distributed data from ozone sondes. The comparisons of SCIAMACHY V2.9 profiles with other satellite datasets are in progress (Rahpoe et al., 2015). In this comparison, 61 ozone sonde stations from the WOUDC (World Ozone and Ultraviolet Radiation Data Centre) as well as SHADOZ (Southern Hemisphere ADditional OZonesondes) databases are involved, covering a wide latitude range from 82.5° N to 70.6° S (see Table 1). The validation includes vertical profile and stratospheric partial column comparisons. In Sect. 2 the algorithms used and the limitations of both SCIAMACHY limb retrievals are discussed. The methodologies of the limb/sonde comparisons are presented in Sect. 3. In Sect. 4 the statistical analysis of the pole to pole comparison results is shown, discussed and summarized.

2 SCIAMACHY limb ozone retrieval

2.1 SCIAMACHY instrument

The SCIAMACHY instrument operated from August 2002 to April 2012 on board the European satellite Envisat (Burrows et al., 1995; Bovensmann et al., 1999). Envisat flied in a sun-synchronous, near-polar orbit with a local equatorial overpass time at around 10 a.m. at the descending node. SCIAMACHY was a passive spectrometer designed to measure radiances in 8 spectral channels covering a wide range from 214 to 2384 nm with a moderate spectral resolution of 0.21 to 1.56 nm. The ozone retrieval algorithm employed in this study uses measurements in the Hartley and Chappuis absorption bands in SCIAMACHY special channels 1 (214–314 nm), 3 (392–605 nm) and 4 (598–790 nm).

AMTD
8, 4817–4858, 2015

SCIAMACHY performed observations in three viewing modes: nadir, limb and solar/lunar occultation. In limb viewing geometry, SCIAMACHY observed the atmosphere with the line of sight pointed tangentially to the Earth's surface, with a field of view of 110 km horizontally and 2.6 km vertically at the tangent point. A limb measurement sequence started from 3 km below the horizon (0 km after October 2010) and continued with a vertical scan up to around 93 km. At each tangent height, SCIAMACHY performed a horizontal scan with a total swath of about 960 km. The horizontal scan is typically read out into 4 measurements with different azimuth angles (only 1 measurement in channel 1). The tangent height step between the subsequent horizontal scans is around 3.3 km. The spatial resolution is typically 960 km × 400 km in channel 1 and 240 km × 400 km (across/along track) in all other channels. The relative azimuth angle between the instrument and the sun changes in course of the orbit. In the high northern latitudes, the instrument measurement field of view faces the solar light with a small relative azimuth angle while in the southern latitudes the solar light comes from behind the instrument field of view and the relative azimuth angle is large.

2.2 SCIAMACHY limb V2.9 retrieval algorithm

The current SCIAMACHY limb retrieval (V2.9) uses combined spectral information from the UV and visible spectral ranges to obtain vertical profiles of ozone (Flittner et al., 2000; Rohen et al., 2006). As the first step, the limb spectral radiances are integrated in ±1 nm intervals around the central points. Then they are normalized with a limb measurement at an upper tangent height (often referred to as the reference tangent height): $I_n(\lambda, \mathrm{TH}_i) = I(\lambda, \mathrm{TH}_i)/I(\lambda, \mathrm{TH}_{\mathrm{ref}})$, with λ denoting wavelength and TH_i the tangent height at the elevation step i. The normalization removes the solar Fraunhofer structures and reduces the influence of the lower atmosphere, e.g. due to multiple scattering and reflection from the surface. Furthermore, it provides a kind of self-calibration of the instrument since the instrument calibration parameters do not differ much for different tangent heights. In the visible spectral range, the so-called triplet method (Flittner et al., 2000) is used subsequently to minimize the influence of the broad-band spectral

Discussion Paper | Discussion Paper | Discussion Paper | Discussion Paper |

AMTD

8, 4817–4858, 2015

Global validation of improved SCIAMACHY scientific ozone limb data

J. Jia et al.

features, e.g. Rayleigh and aerosol scattering. Thereby the measurement vector, $\boldsymbol{y}$, is obtained from the normalized radiances at 525, 589 and 675 nm as follows:

$$\boldsymbol{y}(\mathrm{TH}_i) = \ln(I_n(589\,\mathrm{nm}, \mathrm{TH}_i)) - \frac{1}{2}[\ln(I_n(525\,\mathrm{nm}, \mathrm{TH}_i)) + \ln(I_n(675\,\mathrm{nm}, \mathrm{TH}_i))]. \quad (1)$$

Note that the central wavelength was at 600 nm (center of the Chappuis band) in the original triplet method. It is moved to 589 nm because of issues near the boundary of SCIAMACHY channel 3.

In the UV spectral range the method described by Rohen et al. (2006) is used. The measurement vector, $\boldsymbol{y}$, is obtained from the normalized limb radiance profiles at eight single wavelengths (264, 267.5, 273, 283, 286, 288, 290.5, and 305 nm) with ±1 nm spectral integration (Sonkaew et al., 2009). These wavelengths are chosen to avoid strong Fraunhofer lines and terrestrial airglow emissions. The SCIAMACHY limb ozone profiles are then retrieved by using a non-linear inversion scheme with the first order Tikhonov regularization (Rozanov et al., 2011). The relative change in the ozone concentrations with respect to a priori is retrieved. The forward modelling is done with the radiative transfer model SCIATRAN (Rozanov et al., 2014). The lowest and highest tangent heights used during the retrieval are around 12 and 71 km, respectively.

2.3 SCIAMACHY limb V3.0 retrieval algorithm

In V3.0 retrieval approach, the extra-terrestrial solar spectrum is used instead of the reference tangent height to normalize the measured limb radiances. The differential structure of the ozone absorption signature in the short wavelength wing of the Chappuis absorption band is exploited and the DOAS technique (Platt, 1994) is employed to retrieve the ozone vertical profiles instead of the highly efficient triplet method. These two changes were carried out simultaneously because:

1. The short and long wavelength wings of the Chappuis absorption band are measured in different spectral channels of the SCIAMACHY instrument (see

Sect. 2.1). A usage of the whole Chappuis band in combination with the solar spectrum normalization requires a very high quality of the inter-channel calibration.

2. The signal to noise ratio (SNR) decreases with increasing tangent height. Normalization using reference tangent height at high altitude will reduce the SNR at the corresponding tangent height. Because of the large SNR by using the whole Chappuis band, the signal is sufficient by using reference tangent height. However, differential structure in channel 3 suffers from very low SNR, this influence will be much larger when used without the solar normalization.

Differential limb spectra are obtained as

$$\boldsymbol{y} = \ln(I(\lambda_L, \mathrm{TH}_i)) - P_n, \tag{2}$$

where I is the sun-normalized radiance and P_n is a polynomial of order n (cubic in our case) in λ, whose coefficients are obtained by fitting the logarithms of the normalized limb radiance in the wavelength domain for each tangent height independently. A shift and squeeze correction as well as scaling factors for Ring and water vapour absorption spectra are determined at each tangent height. The shift and squeeze correction is done with respect to the limb measured spectrum for both the modelled spectra and the measurement at the reference tangent height (Rozanov et al., 2005).

Since the ozone absorption signature from the short wavelength differential absorption cross section structures of the Chappuis absorption band are weaker than the differences of the absorption between the 3 wavelength used in the triplet Chappuis band, the influence of weaker absorbers, namely, NO_2 and O_4 needs to be taken into account. The wavelength dependence of the surface albedo spectral reflectance is also included in the fit. The mathematical inversion then proceeds in a manner similar to that used in V2.9 retrieval (Rozanov et al., 2007). In V3.0 retrieval approach, the full spectrum of the UV band (229–306) with zero order polynomial is used instead of the selected wavelengths as in V2.9. This however does not play any role in the comparison with the vertical profile of ozone from ozone sondes discussed in this manuscript as the information from the UV range does not have any significant influence on the retrieved ozone values below 30 km. The lowest and highest tangent heights used during this retrieval are around 8 and 65 km, respectively.

2.4 Limb ozone data

The IUP Bremen Level 2 product provides ozone data as number densities in molecules cm^{-3} and as volume mixing ratios in ppmV vs. altitude within each ground pixel. The product also contains the corresponding a priori ozone profiles as well as error estimates in both number density and volume mixing ratio representations. Cloud information is retrieved by using SCODA (SCIAMACHY Cloud Detection Algorithm) data base (Eichmann et al., 2011) and is provided as "cloud flag" in the data. In the V3.0 data product, the vertical resolution is added. The vertical resolution S_i is calculated from the spread of the averaging kernels (Backus and Gilbert, 1970) as:

$$S_i = 12 \cdot \sum_j A_{ij}^2 \cdot (Z_j - Z_i)^2 \cdot \Delta Z_j \Big/ \left(\sum_j A_{ij} \cdot \Delta Z_j \right)^2, \quad (3)$$

where i represents the elevation step, Z is the altitude, and A_{ij} refers to the corresponding element of the averaging kernel matrix. To perform the integration, the averaging kernels need to be re-sampled to a finer grid. In this study 20 sub-layers are used. Although the vertical resolution is not included in the V2.9 data products, in this study we calculate it in the same way as for V3.0 for the purpose of data selection (see Sect. 3.1.2). Examples of the averaging kernels, measurement response as well as vertical resolution resulting from both V2.9 and V3.0 are given in Fig. 1. As the retrieval is done at the measurement tangent heights, the averaging kernels for V3.0 reach a value of 1.0 at the maxima between 12 and 60 km. For V2.9 the value is around 0.3, which is due to the retrieval at finer grid (1 km) compared to the measurement grid (∼ 3 km). Measurement response is calculated by summing the elements of the corresponding

Discussion Paper | Discussion Paper | Discussion Paper | Discussion Paper |

AMTD

8, 4817–4858, 2015

Global validation of improved SCIAMACHY scientific ozone limb data

J. Jia et al.

averaging kernel. It describes how much information comes from the measurement. Measurement response indicates that

1. The retrieved profile is completely independent from the a priori information within the whole altitude range for V3.0 and above 12 km for V2.9.
2. Below 12 km V2.9 may contain less information from the measurement and is stronger affected by the a priori information compared to V3.0. (Note that V3.0 uses measurement down to 8 km, while V2.9 stops at 12 km.)

From the vertical resolution we observe: at the altitudes above 65 km profile information comes from 60–70 km altitude range for both data sets; information below 12 km partially originates from the upper layers for both versions.

3 Validation methodologies

To validate the scientific ozone profiles retrieved from SCIAMACHY limb measurements, ozone sonde data from WOUDC stations are used. In order to select a reliable reference data set, only stations that have delivered more than 30 measurements between January 2003 and December 2012 are selected for the comparisons. Coincident SCIAMACHY limb profiles are selected for each ozone sonde profile. The geographic distance between the ozone sonde station and the footprint centre of the co-located SCIAMACHY measurement is required to be within 5° in latitude and 10° in longitude. A maximum data, have the time difference of the measurements of less than or equal to 24 h, are used. The coincident limb profiles having a solar zenith angle larger than 80 °, in general, an altitude range between 15–30 km is selected for the partial column comparison (See Sect. 3.2). This choice is motivated by larger uncertainties of the current limb retrievals below 15 km and increasing uncertainty in the ozone sonde data above 30 km. The latter is mostly caused by the decaying pump efficiency at lower pressures (Johnson et al., 2002).

AMTD
8, 4817–4858, 2015

In the 61 ozone sonde stations that were used, 14 stations are from the tropics, 31 stations are from northern mid-latitudes, 6 stations are from northern high latitudes, 6 stations are from southern mid-latitudes and 4 stations are from southern high latitudes (see Table 1).

3.1 Vertical profiles

3.1.1 Convolution of ozone sonde data

Satellite data has a much coarser vertical resolution compared to the ozone sondes. To make a quantitative comparison, SCIAMACHY averaging kernels, A, and a-priori information, X_a, are used to degrade high vertical resolution sonde data to the vertical resolution of the satellite data. This represents the profiles from ozone sondes as they should be seen by the satellite retrieval in the absence of any errors which are not accounted for by the retrieval. The smoothed ozone sonde profile, X_si, is obtained from the fine profile, X_sj, by convolving with the SCIAMACHY averaging kernels as:

$$\frac{X_\mathrm{si}-X_\mathrm{ai}}{X_\mathrm{ai}} = \left(\sum_j \Delta Z_j\right)^{-1} \cdot \sum_j A_{ij} \cdot \frac{X_\mathrm{sj}-X_\mathrm{aj}}{X_\mathrm{aj}} \cdot \Delta Z_j, \tag{4}$$

where i represents the satellite coarse grid, j the fine grid of the ozone sonde; the rows of the averaging kernel matrix and a-priori profile are interpolated to the ozone sonde grid and represented by A_{ij} and X_aj respectively; ΔZ_j is the altitude interval, i.e. a half distance between the layers above and below j. For each level of the coarse grid, i, the smoothed ozone sonde value

$$X_\mathrm{si} = X_\mathrm{ai} \cdot \left(\sum_j \Delta Z_j\right)^{-1} \cdot \sum_j A_{ij} \cdot \frac{X_\mathrm{sj}-X_\mathrm{aj}}{X_\mathrm{aj}} \cdot \Delta Z_j + X_\mathrm{ai}, \tag{5}$$

AMTD
8, 4817–4858, 2015

3.1.2 Layer selection criteria

Two criteria were defined to screen proper vertical layers before the comparisons. Firstly, all averaging kernels used for the convolution (see Eq. 5) must not have non-zero elements above the maximum height of the corresponding ozone sonde measurement. Secondly, all layers below the cloud top height, as detected by the SCODA algorithm, are rejected, altitude grid points, where the resulting vertical resolution is lower than 6 km, are also not considered.

V3.0 profiles are retrieved at the measurement grid, which varies depending on the location and time. When calculating the mean differences between ozone sonde data and V3.0 limb data at each elevation step, initially an averaged altitude between January 2003 and December 2011 is calculated. Then each single profile is interpolated to the average altitude grid in each layer. At each layer the selected ozone profiles are averaged, denoted as $\overline{C_{\mathrm{SCIA}}}$ and $\overline{C_{\mathrm{ref}}}$. The relative mean difference at each layer is calculated as:

$$D = \frac{\overline{C_{\mathrm{SCIA}}} - \overline{C_{\mathrm{ref}}}}{\overline{C_{\mathrm{ref}}}} \cdot 100\,\%. \tag{6}$$

The corresponding SD is given by:

$$\mathrm{Dev} = \sqrt{\frac{1}{k-1}\sum_{i=1}^{k}\left(AC(i) - \overline{AC}(i)\right)^2} \cdot 100\,\%. \tag{7}$$

where k is the number of profiles included in the comparison and

$$AC(i) = (C_{\mathrm{SCIA}}(i) - C_{\mathrm{ref}}(i))/\overline{C_{\mathrm{ref}}}. \tag{8}$$

$$\overline{AC}(i) = D = \frac{1}{k}\sum_{i=1}^{k} AC(i). \tag{9}$$

AMTD
8, 4817–4858, 2015

3.2 Partial column comparisons

In addition to the vertical profile comparison, both SCIAMACHY limb ozone data and original ozone sonde measurements are integrated and compared as the stratospheric partial ozone columns (hereafter SC). For each individual pair of SCIAMACHY/sonde profiles, the integration is started either from the first cloud-free level of SCIAMACHY limb data or from 15 km, whichever is higher, and ended at either the ozone sonde explosion position or at 30 km, whichever is lower.

$$C_{\text{strato}} = \sum_{i_{\text{tph}}}^{i=\text{TH}_{\text{max}}} \left(\frac{N(Z_{i-1}) + N(Z_i)}{2} \right) (Z_i - Z_{i-1}). \tag{10}$$

where C_{strato} refers to a individual SC, $N(z)$ is the stratospheric ozone profile in number density units (mol cm^{-3}), z_i represents the altitude in km and i is the layer index.

4 Results and discussion

4.1 Vertical profile comparison results for V2.9 and V3.0

Average vertical profiles from the six selected stations for a period January 2003–December 2011 are compared in Figs. 2–7. The stations Nairobi, Ankara, Praha, Eureka, Lauder and Marambio are chosen as representatives of the latitude bins 20° S–20° N, 20–40° N, 40–60° N, 60–90° N, 20–60° S, 60–90° S, respectively. The panels represent the results of V2.9 on the left hand side and of V3.0 on the right hand. For each station, the vertical comparisons are shown as vertical profiles (left panels) and relative mean differences (right panels). The number densities for both sonde and SCIAMACHY limb data at each layer are obtained by averaging the filtered data (see Sect. 3.1.2) over the entire time period. At Nairobi (Fig. 2), V2.9 agrees with ozone sonde results to within 3 % for most cases below 30 km. There are good agreements at Ankara (Fig. 3), Lauder (Fig. 6) and Marambio (Fig. 7) with usually less than 5 % relative differences. The differences become larger at Lauder below 18 km. A negative bias shows up at Praha (Fig. 4) and becomes stronger at Eureka (Fig. 5), which has higher latitude. Furthermore, the relative differences at these latitudes exhibit vertical oscillations of about 3 % amplitude. The maxima of the relative differences are seen at around 22 and 28 km. The oscillations are most probably caused by the fact that: the radiance profiles, sampled by the SCIAMACHY instrument at different tangent heights, are not exactly aligned vertically (Brinksma et al., 2006). At these latitudes, the horizontal variations of the stratospheric ozone are usually stronger as compared to other latitudes and thus the oscillations are more pronounced.

To give a global overview of the results, the altitude vs. latitude cross sections of the relative differences for both versions are given in Fig. 8. They are calculated by contouring the relative mean differences between SCIAMACHY limb data and correlative sonde data at all considered sonde stations (61 stations in total). In general, the current V2.9 data well reproduce the ozone vertical distribution by following the shapes of ozone sonde data at each station (upper panel of Fig. 8). The relative differences between V2.9 and ozone sonde data are within 5 % between 20–30 km southward of 40° N. The good agreement seen at Nairobi holds for most of the cases in the tropical region. One exception is seen around the ozone peak altitude (∼ 26 km) in the near-equatorial northern tropics. This overestimation can be clearly observed (not shown in this paper) at Sepang-Airport (Kuala Lumpur) and Hong Kong stations with more than 10 % relative differences in the upper stratosphere (25 to 30 km). In the middle and high southern latitudes, V2.9 still represents the ozone vertical distribution very well by agreeing with ozone sonde data to within 5 % which is consistent with Figs. 3, 6 and 7. In the Northern Hemisphere, this consistent agreement degrades northward of ∼ 40° N, showing stronger underestimation with increasing latitude up to ∼ 15 %. The oscillations we see in Figs. 4 and 5 can be observed, too.

The vertical profile comparison results from upcoming V3.0 data sets are presented in the lower panel of Fig. 8 in the same way as for V2.9. In comparison to the current

AMTD
8, 4817–4858, 2015

V2.9 data sets, V3.0 shows similar retrieval quality in most of the cases with exception of a slightly worse agreement at Nairobi (shown in the panel of Fig. 2–7), while the overestimations over the Southeast Asia (e.g. Kuala Lumpur, Hong Kong) in V2.9 are revised (Fig. 8). It is seen clearly that the ozone concentrations at mid and high northern latitudes, e.g. Praha and Eureka, are captured more accurately in V3.0 than in V2.9. For example, at Eureka the relative differences are reduced from ~ 13 to within 7.5 %. The vertical oscillations can still be observed but are much weaker. V3.0 agrees with ozone sonde within 10 % globally, with a significant improvement northwards of 40° N (Fig. 8).

Figures 9 and 10 show annual and seasonal relative differences for V2.9, respectively. The relative mean differences at all tropical (not shown in the paper) and mid latitude stations don't have much dependence on the year of measurements. However, the relative differences drift from year to year at high latitudes of both hemispheres (see Fig. 9). The statistics of the seasonal behaviour is presented in Fig. 10. No obvious seasonal influence can be identified in this comparison. Since V3.0 has a similar seasonal and yearly behaviour (apart from the reduced bias at Eureka and Praha) of the vertical profiles as V2.9, the results are not shown.

4.2 Partial column comparison results for V2.9 and V3.0

The results of partial column comparisons are presented in Figs. 11–18. Figure 11 depicts the time series of ozone sonde data sets (red dots), SCIAMACHY data sets (green dots) and their differences (blue dots) at Nairobi and Eureka. The ozone amounts are represented as daily averaged SCs in DU. The left panels represent the current V2.9, while the right ones the upcoming V3.0. Figures 12–18 show the statistical results for the differences of SCs in DU between the ozone sonde and the SCIAMACHY data on a global scale. Figure 12 shows the global overview of the absolute and relative averaged daily differences while Figs. 13–18 presents scatter plots of the absolute differences for latitude bins. Note that the absolute differences in Fig. 12 are calculated

AMTD
8, 4817–4858, 2015

as the averages of the daily mean SCs differences while in Figs. 13–18 each dot represents the absolute difference for a single collocation.

Similar conclusions as for the vertical profile comparisons can be drawn from the partial column comparisons. For V2.9 data set, the seasonal variations in the time series agree well with those from sonde data (left panels of Fig. 11). The drift of relative differences with time that is mentioned in Sect. 4.1 can be observed also in Fig. 11 at Eureka. So far there is no explanation about this drift. The agreement of daily mean differences is mostly within 5 DU southwards from 40° N. The overestimation in Southeast Asia observed in Fig. 8 corresponds to ~ 10 DU absolute differences as shown in Fig. 12. A general overestimation in the Pacific Ocean can also be observed. In the northern middle and high latitudes, a rapid decrease in the quality of the V2.9 ozone data results in, e.g., a median difference of 22 DU (over 10 %) at Eureka. The underestimations are depicted by the purple and pink dots in Fig. 12 and amount about ~ 13 DU in Europe and Canada and more than 20 DU in the high northern latitudes.

For V3.0, the seasonal variations in the time series are in good agreement with those from sonde data; at Eureka a median difference in partial columns decreases by 16 DU to only 6 DU (right panel of Fig. 11). The improvement northwards of 40° N changes the color in Fig. 12, from purple pink to blue. V3.0 also improved the partial column accuracy at most tropical stations (10 out of 12 stations with abundant measurements) with a remarkable ~ 5 % improvement from more than 8 to within 4 % over the tropical Pacific region.

A global improvement can be observed in the statistical results for different latitude bins (Figs. 13–18) illustrating better retrieval results for each single measurement. A striking improvement is seen in the high latitude bin (60–90° N). With an improved linear slope of 0.94 vs. 0.85 and smaller SD of σ = 7.4 DU vs. 13.7 DU, V3.0 data set exhibits a much better agreement with ozone sonde data at northern high latitudes. At the same time, the correlations at other latitude bins also become higher in varying degrees. A very strong improvement can be observed also in southern mid latitudes

AMTD
8, 4817–4858, 2015

(Fig. 16). Due to the relatively low and centred ozone partial column, a smaller correlation is obtained in the tropics for both versions.

4.3 Discussions

The reasons for the underestimation found in V2.9 data at higher latitudes can be identified by analysing the left panel of Fig. 19. The figure shows a comparison of ozone vertical profiles from SCIAMACHY V2.9 data (blue solid line) and from ozone sonde (black solid line) at Eureka for 22 March 2006. A clear underestimation of the peak value near 17 km is observed in V2.9 data. This is a typical behaviour that explains the underestimation described above. As this artifact could not be reproduced in the synthetic retrievals it is most probably caused by instrumental issues. One possible explanation is a presence of an increased external stray light when performing limb measurements at large solar zenith angles and small azimuth angles. In this geometry, which is typical for SCIAMACHY observations at high northern latitudes, the extraterrestrial solar radiance is believed to be reflected by some part of the Envisat into the field of view of the SCIAMACHY instrument.

The retrieval methodology used in the new V3.0 aims to reduce the underestimations in the northern high latitudes shown by V2.9. In the V3.0 retrieval processor, signals from different wavelengths are exploited (Sect. 2.3). The spectral window used in the visible region is narrower compared to V2.9. On one hand it uses weaker absorption features of ozone gaining thus less information from the spectra. On the other hand, by using the narrow spectral window and higher order of the closure polynomial the influence of the systematic errors is reduced. The right panel of Fig. 19 shows the comparison of ozone vertical profiles from SCIAMACHY limb V3.0 data with ozone sonde data presented in the same way as V2.9 results in the left panel. It is seen clearly that the ozone maximum at 17 km observed by the sonde is now captured properly by SCIAMACHY. Furthermore, V3.0 data set also reproduces better the ozone maximum around 25 km in the tropics (not shown here), which corrects the overestimation in Southeast Asia as seen from both vertical and partial column comparisons. General

AMTD
8, 4817–4858, 2015

Global validation of improved SCIAMACHY scientific ozone limb data

J. Jia et al.

improvement in the Pacific and the Southern Atlantic ocean regions can be observed in the partial column comparisons (Fig. 12). This may be partly due to the opposite sign of differences at different altitude. As shown in the sections above, the new V3.0 is a success in solving the northern high latitudes underestimation.

5 Conclusions

SCIAMACHY limb ozone scientific data sets, namely the current V2.9 and the new V3.0, were extensively compared with ozone sonde measurements for the time period of 2003–2011, from 61 sonde stations. The two versions of SCIAMACHY limb data use different retrieval processors. The main differences are: in visible spectral region V2.9 uses a reference tangent height and the triplet method while V3.0 employs a solar spectrum as the reference and performs a DOAS type fit. There are also some changes in the UV band (Sects. 2.2 and 2.3), these however do not provide information at altitudes less than 30 km.

V2.9 agrees well with the ground based data within a latitude range of 90° S–40° N. The relative differences between the two databases are within 5 % (SCIAMACHY is mostly overestimating) at 20–30 km. It shows very good retrieval results in the tropics with a difference of less than 3 % vertically. The partial column comparisons show less than 5 DU absolute differences with rather small SD with exception of the tropical Pacific region where an overestimation of more than 10 % is observed. These overestimations result from a significant positive bias above 25 km (so far there is no explanation for the reason of this bias). In the northern high latitudes V2.9 shows up to ∼ 15 % negative bias with observable vertical oscillations, which is believed to be the consequences of the increased external stray light. The ozone partial columns are underestimated by 12–20 DU.

The new V3.0 has been developed to reduce the underestimation in the northern high latitude identified in V2.9. As a result the differences are reduced to within 10 % for vertical profiles and 5 to 10 DU for partial columns northward of 40° N. At the same

AMTD
8, 4817–4858, 2015

time, the overestimation of the ozone profile concentrations around tropical Pacific are eliminated. We show that V3.0 maintains the good retrieval results also southwards of 40° N, with deviations slightly larger than 5 % in the tropics and within 10 % in the southern high latitude.

The Huggins band is believed to improve ozone retrieval accuracy between 30 km-45 km and will be included in V3.1 limb ozone retrieval.

Acknowledgements. We acknowledge WOUDC (http://woudc.org) for providing ozone sonde datasets. We acknowledge the GALAHAD Fortran library used for V3.0 retrieval (Gould et al., 2003). Jia Jia acknowledges funding by CSC (China Scholarship Council). We also acknowledge financial support provided by ESSReS (Earth System Science Research School) and the BMBF ROMIC project. This work has also been funded in parts by the German Aerospace DLR project SADOS(FKZ 50EE1105) and by the University and State of Bremen. We thank the colleagues for continuing support and discussion.

The article processing charges for this open-access publication were covered by the University of Bremen.

References

Backus, G. E. and Gilbert, F. E.: Uniqueness in the inversion of inaccurate gross Earth data, Philos. T. Roy. Soc. A, 266, 1173, 123–192, 1970.

Bovensmann, H., Burrows, J. P., Buchwitz, M., Frerick, J., Noël, S., Rozanov, V. V., Chance, K. V., and Goede, A. P. H.: SCIAMACHY: mission objectives and measurement modes, J. Atmos. Sci., 56, 127–150, 1999.

Brinksma, E. J., Bracher, A., Lolkema, D. E., Segers, A. J., Boyd, I. S., Bramstedt, K., Claude, H., Godin-Beekmann, S., Hansen, G., Kopp, G., Leblanc, T., McDermid, I. S., Meijer, Y. J., Nakane, H., Parrish, A., von Savigny, C., Stebel, K., Swart, D. P. J., Taha, G., and Piters, A. J. M.: Geophysical validation of SCIAMACHY Limb Ozone Profiles, Atmos. Chem. Phys., 6, 197–209, doi:10.5194/acp-6-197-2006, 2006.

Burrows, J., Hölzle, E., Goede, A., Visser, H., and Fricke, W.: SCIAMACHY – scanning imaging absorption spectrometer for atmospheric chartography, Acta Astronaut., 35, 445–451, 1995.

AMTD

8, 4817–4858, 2015

Eichmann, K.-U., von Savigny, C., Weigel, K., Reichl, P., Robert, C., Steinwagner, J., Bovensmann, H., and Burrows, J. P.: SCODA V1.9: SCIAMACHY Cloud Detection Algorithm from Limb Radiance Measurements, Algorithm Theoretical Baseline Document (ATBD), University of Bremen, Bremen, Germany, 2011.

Flittner, D. E., Bhartia, P. K., and Herman, B. M.: O_3 profiles retrieved from limb scatter measurements: theory, Geophys. Res. Lett., 27, 2601–2604, 2000.

Gould, N. I. M., Orban, D., and Toint, P. L.: GALAHAD, a library of thread-safe Fortran 90 packages for large-scale nonlinear optimization, ACM T. Math. Software, 29, 353–372, 2003.

Hassler, B., Petropavlovskikh, I., Staehelin, J., August, T., Bhartia, P. K., Clerbaux, C., Degenstein, D., Mazière, M. De, Dinelli, B. M., Dudhia, A., Dufour, G., Frith, S. M., Froidevaux, L., Godin-Beekmann, S., Granville, J., Harris, N. R. P., Hoppel, K., Hubert, D., Kasai, Y., Kurylo, M. J., Kyrölä, E., Lambert, J.-C., Levelt, P. F., McElroy, C. T., McPeters, R. D., Munro, R., Nakajima, H., Parrish, A., Raspollini, P., Remsberg, E. E., Rosenlof, K. H., Rozanov, A., Sano, T., Sasano, Y., Shiotani, M., Smit, H. G. J., Stiller, G., Tamminen, J., Tarasick, D. W., Urban, J., van der A, R. J., Veefkind, J. P., Vigouroux, C., von Clarmann, T., von Savigny, C., Walker, K. A., Weber, M., Wild, J., and Zawodny, J. M.: Past changes in the vertical distribution of ozone – Part 1: Measurement techniques, uncertainties and availability, Atmos. Meas. Tech., 7, 1395–1427, doi:10.5194/amt-7-1395-2014, 2014.

Johnson, B. J., Oltmans, S. J., Vömel, H., Smit, H. G. J., Deshler, T., and Kroger, C.: Electrochemical concentration cell (ECC) ozone sonde pump efficiency measurements and tests on the sensitivity to ozone of buffered and unbuffered ECC sensor cathode solutions, J. Geophys. Res., 107, 4393, 2002.

Mieruch, S., Weber, M., von Savigny, C., Rozanov, A., Bovensmann, H., Burrows, J. P., Bernath, P. F., Boone, C. D., Froidevaux, L., Gordley, L. L., Mlynczak, M. G., Russell III, J. M., Thomason, L. W., Walker, K. A., and Zawodny, J. M.: Global and long-term comparison of SCIAMACHY limb ozone profiles with correlative satellite data (2002–2008), Atmos. Meas. Tech., 5, 771–788, doi:10.5194/amt-5-771-2012, 2012.

Platt, U.: Differential optical absorption spectroscopy (DOAS), Chem. Anal. Series, 127, 27–83, 1994.

Rahpoe, N., von Savigny, C., Weber, M., Rozanov, A.V., Bovensmann, H., and Burrows, J. P.: Error budget analysis of SCIAMACHY limb ozone profile retrievals using the SCIATRAN model, Atmos. Meas. Tech., 6, 2825–2837, doi:10.5194/amt-6-2825-2013, 2013.

AMTD

8, 4817–4858, 2015

Global validation of improved SCIAMACHY scientific ozone limb data

J. Jia et al.

Rahpoe, N., Weber, M., Rozanov, A. V., Weigel, K., Bovensmann, H., Burrows, J. P., Laeng, A., Stiller, G., von Clarmann, T., Kyröla, E., Sofieva, V. F., Tamminen, J., Walker, K., Degenstein, D., Bourassa, A. E., Hargreaves, R., Bernath, P., Urban, J., and Murtagh, D. P.: Relative drifts and biases between six ozone limb satellite measurements from the last decade, Atmos. Meas. Tech. Discuss., 8, 3697–3728, doi:10.5194/amtd-8-3697-2015, 2015.

Read, P. L.: Theory of planetary atmospheres: an introduction to their physics and chemistry. (2nd edition). By J. W. Chamberlain and D. M. Hunten. International Geophysics Series, 36. Academic Press Inc. Florida. 1987. Pp. 481. £41.50, Q. J. Roy. Meteor. Soc., 114, 551–552, doi:10.1002/qj.49711448014, 1988.

Rohen, G. J., von Savigny, C., Llewellyn, E. J., Kaiser, J. W., Eichmann, K.-U., Bracher, A., Bovensmann, H., and Burrows, J. P.: First results of ozone profiles between 35 and 65 km retrieved from SCIAMACHY limb spectra and observations of ozone depletion during the solar proton events in Oct./Nov. 2003, Adv. Space Res., 37, 2263–2268, 2006.

Rozanov, A., Bovensmann, H., Bracher, A., Hrechanyy, S., Rozanov, V., Sinnhuber, M., Stroh, F., and Burrows, J. P.: NO_2 and BrO vertical profile retrieval from SCIAMACHY limb measurements: sensitivity studies, Adv. Space Res., 36, 846–854, 2005.

Rozanov, A., Eichmann, K.-U., von Savigny, C., Bovensmann, H., Burrows, J. P., von Bargen, A., Doicu, A., Hilgers, S., Godin-Beekmann, S., Leblanc, T., and McDermid, I. S.: Comparison of the inversion algorithms applied to the ozone vertical profile retrieval from SCIAMACHY limb measurements, Atmos. Chem. Phys., 7, 4763–4779, doi:10.5194/acp-7-4763-2007, 2007.

Rozanov, A., Kühl, S., Doicu, A., McLinden, C., Puķīte, J., Bovensmann, H., Burrows, J. P., Deutschmann, T., Dorf, M., Goutail, F., Grunow, K., Hendrick, F., von Hobe, M., Hrechanyy, S., Lichtenberg, G., Pfeilsticker, K., Pommereau, J. P., Van Roozendael, M., Stroh, F., and Wagner, T.: BrO vertical distributions from SCIAMACHY limb measurements: comparison of algorithms and retrieval results, Atmos. Meas. Tech., 4, 1319–1359, doi:10.5194/amt-4-1319-2011, 2011.

Rozanov, V., Rozanov, A., Kokhanovsky, A., and Burrows, J.: Radiative transfer through terrestrial atmosphere and ocean: software package SCIATRAN, J. Quant. Spectrosc. Ra., 133, 13–71, 2014.

Sofieva, V. F., Rahpoe, N., Tamminen, J., Kyrölä, E., Kalakoski, N., Weber, M., Rozanov, A., von Savigny, C., Laeng, A., von Clarmann, T., Stiller, G., Lossow, S., Degenstein, D., Bourassa, A., Adams, C., Roth, C., Lloyd, N., Bernath, P., Hargreaves, R. J., Urban, J., Murtagh, D., Hauchecorne, A., Dalaudier, F., van Roozendael, M., Kalb, N., and Zehner, C.:

Harmonized dataset of ozone profiles from satellite limb and occultation measurements, Earth Syst. Sci. Data, 5, 349–363, doi:10.5194/essd-5-349-2013, 2013.
Sonkaew, T., Rozanov, V. V., von Savigny, C., Rozanov, A., Bovensmann, H., and Burrows, J. P.: Cloud sensitivity studies for stratospheric and lower mesospheric ozone profile retrievals from measurements of limb-scattered solar radiation, Atmos. Meas. Tech., 2, 653–678, doi:10.5194/amt-2-653-2009, 2009.
Tegtmeier, S., Hegglin, M. I., Anderson, J., Bourassa, A., Brohede, S., Degenstein, D., Froidevaux, L., Fuller, R., Funke, B., Gille, J., Jones, A., Kasai, Y., Krüger, K., Kyrölä, E., Lingenfelser, G., Lumpe, J., Nardi, B., Neu, J., Pendlebury, D., Remsberg, E., Rozanov, A., Smith, L., Toohey, M., Urban, J., von Clarmann, T., Walker, K. A., and Wang, R. H. J.: SPARC Data Initiative: a comparison of ozone climatologies from international satellite limb sounders, J. Geophys. Res.-Atmos., 118, 12229–12247, 2013.

Table 1. WOUDC and SHADOZ stations used in the validation.

Station Name	Height [m]	Country	Latitude	Longitude
NH high latitude				
Alert	66	CAN	82.5° N	62.3° W
Eureka	10	CAN	80.0° N	85.9° W
Lerwick	80	GBR	60.1° N	1.2° W
Ny-Aalesund	11	NOR	78.9° N	11.9° E
Resolute	46	CAN	74.7° N	94.9° W
Sodankyla	179	FIN	67.4° N	26.6° E
NH mid latitude				
Ankara	890	TUR	39.9° N	32.8° E
Barajas	631	ESP	40.4° N	3.5° W
BrattsLake	580	CAN	50.2° N	104.7° W
Churchill	30	CAN	58.7° N	94.1° W
DeBilt	4	NLD	52.1° N	5.1° E
Egbert	251	CAN	44.2° N	79.7° W
Hohenpeissenberg	976	DEU	47.8° N	11° E
Holtville[a]	−19	USA	32.8° N	115.3° W
HongKong	66	HKG	22.3° N	114.1° E
Houston	19	USA	29.7° N	95.4° W
Huntsville	196	USA	34.7° N	86.6° W
Isfahan	1550	IRN	32.5° N	51.7° E
Kelowna	456	CAN	49.9° N	119.4° W
Legionowo	96	POL	52.4° N	20.9° E
Naha	28	JPN	26.2° N	127.6° E
Narragansett	21	USA	41.4° N	71.4° W
Payerne	491	CHE	46.5° N	6.5° E
Praha	304	CZE	50.0° N	14.4° E
Richland[a]	123	USA	46.2° N	119.1° W
SableIsland	4	CAN	43.9° N	60.0° W
Sapporo	26	JPN	43.0° N	141.3° E
Stonyplain	766	CAN	53.5° N	114.1° W
TableMountain	2285	USA	34.4° N	117.7° W
TrinidadHead	20	USA	40.8° N	124.1° W
Tsukuba	31	JPN	36.0° N	140.1° E
Uccle	100	BEL	50.8° N	4.3° E
ValentiaObservatory	14	IRL	51.9° N	10.2° W
Valparaiso[a]	240	USA	41.5° N	87° W
WallopsIsland	13	USA	37.9° N	75.4° W
Walsingham	200	CAN	42.6° N	80.6° W
Yarmouth	9	CAN	43.8° N	66.1° W

AMTD
8, 4817–4858, 2015

Table 1. Continued.

Station Name	Height [m]	Country	Latitude	Longitude
Tropics				
Alajuela[b]	899	CRI	9.9° N	84.2° W
AscensionIsland[b]	79	SHN	7.9° S	14.4° W
Barbados[a,b]	32	BRB	13.1° N	59.4° W
Heredia[b]	1176	CRI	10° N	84.1° W
Hilo[b]	2994	USA	19.4° N	155.0° W
Malindi[b]	−6	KEN	3.0° S	40.2° E
Maxaranguape (Natal)[b]	14	BRA	5.5° S	35.2° W
Nairobi[b]	1795	KEN	1.2° S	36.8° E
Paramaribo[b]	7	SUR	5.8° N	55.2° W
Samoa[b]	77	ASM	14.2° S	170.5° W
SanCristobal[b]	8	ECU	0.9° S	89.6° W
SepangAirport[b]	17	MYS	2.7° N	101.7° E
Tecamec[b]	2272	MEX	19.3° N	99.1° W
Watukosek (Java)[b]	50	IDN	7.5° S	112.6° E
SH mid latitude				
Broadmeadows	109	AUS	37.7° S	144.9° E
Irene[b]	1524	ZAF	25.9° S	28.2° E
LaReunionIsland[b]	24	REU	21.0° S	55.4° E
Lauder	370	NZL	45.0° S	169.6° E
MacquarieIsland	7	AUS	54.5° S	158.9° E
Ushuaia	17	ARG	54.8° S	68.3° W
Antarctic				
Davis	18	ATA	68.5° S	77.9° E
Marambio	198	ATA	64.2° S	56.6° W
Neumayer	38	ATA	70.6° S	8.2° W
Syowa	22	JPN	69.0° S	39.5° E

[a] stations with less than 30 ozone sonde profiles.
[b] stations originally from SHADOZ

AMTD
8, 4817–4858, 2015

Global validation of improved SCIAMACHY scientific ozone limb data

J. Jia et al.

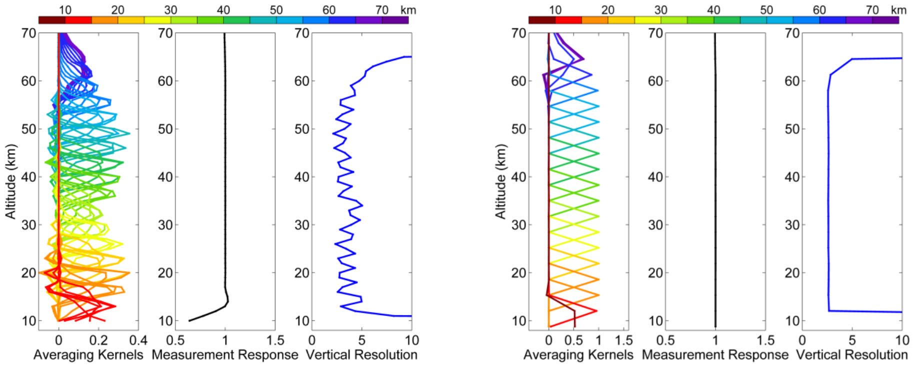

Figure 1. Averaging kernels, measurement response as well as vertical resolution from SCIAMACHY V2.9 (left panel) and V3.0 (right panel). Note that the *x* axis range is different between the two panels. The example is calculated for orbit 21223; measured at 17:36 UTC on 22 March 2006; solar zenith angle @ TP 74.95; at 75.44° N and 93.58° W.

AMTD
8, 4817–4858, 2015

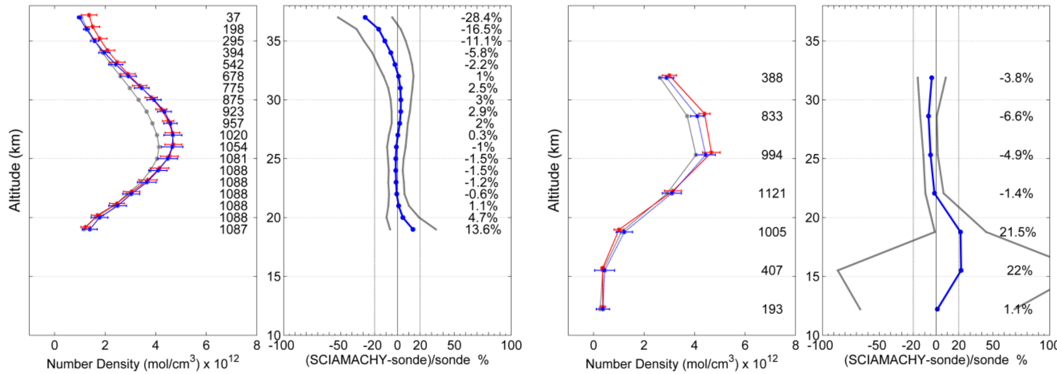

Figure 2. Vertical profile comparisons at Nairobi (1.2° N, 36.8° E) averaged from January 2003 to December 2012. The 4 panels show the results for the ozone profiles for V2.9 on the left hand side and for V3.0 on the right hand. In the left subpanels, the red and blue curves represent the ozone number densities with 1σ SDs for ozone sonde and SCIAMACHY limb data, respectively. The gray lines show a priori information used in SCIAMACHY retrieval. In the right subpanels, the blue lines represent the relative mean differences of the ozone concentrations. The gray solid lines depict 1σ SDs. The numbers on the right denote the number of SCIAMACHY limb profiles used in the comparisons and the relative differences for each layer, respectively.

AMTD
8, 4817–4858, 2015

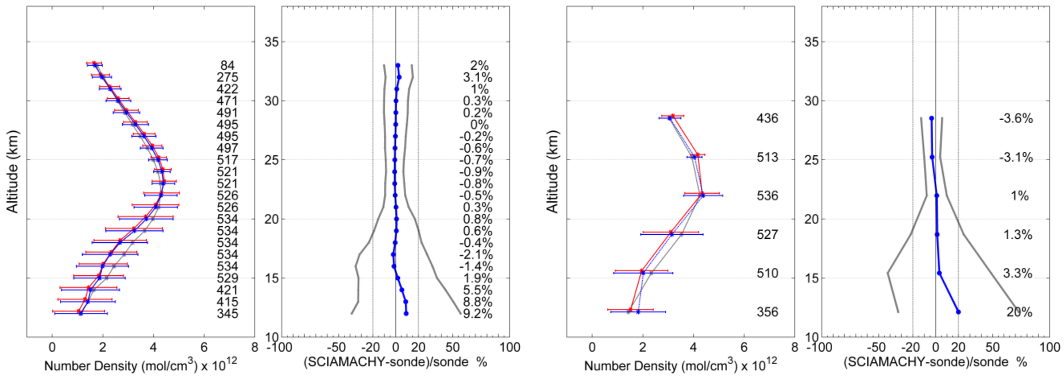

Figure 3. Same as Fig. 2 but for Ankara (40.0° N, 32.8° E).

AMTD
8, 4817–4858, 2015

Global validation of improved SCIAMACHY scientific ozone limb data

J. Jia et al.

Title Page
Abstract | Introduction
Conclusions | References
Tables | Figures
◀| |▶
◀ ▶
Back | Close
Full Screen / Esc
Printer-friendly Version
Interactive Discussion

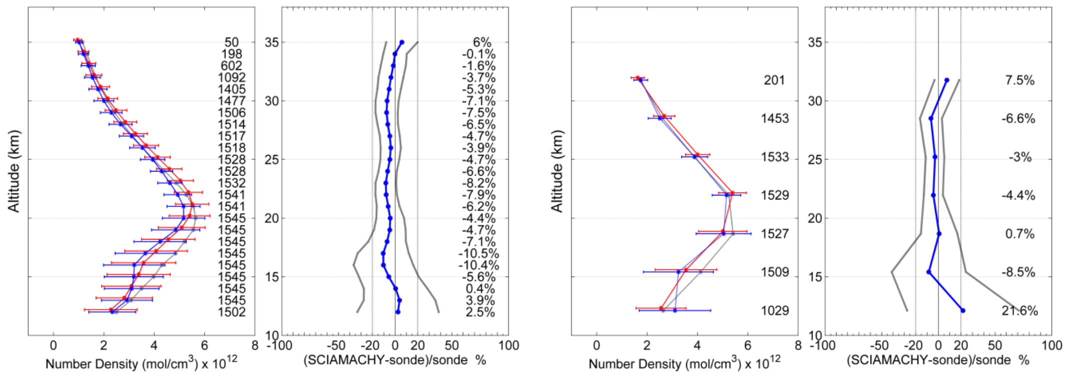

Figure 4. Same as Fig. 2 but for Praha (50.0° N, 14.4° E).

AMTD
8, 4817–4858, 2015

Global validation of improved SCIAMACHY scientific ozone limb data

J. Jia et al.

Title Page
Abstract Introduction
Conclusions References
Tables Figures
Back Close
Full Screen / Esc
Printer-friendly Version
Interactive Discussion

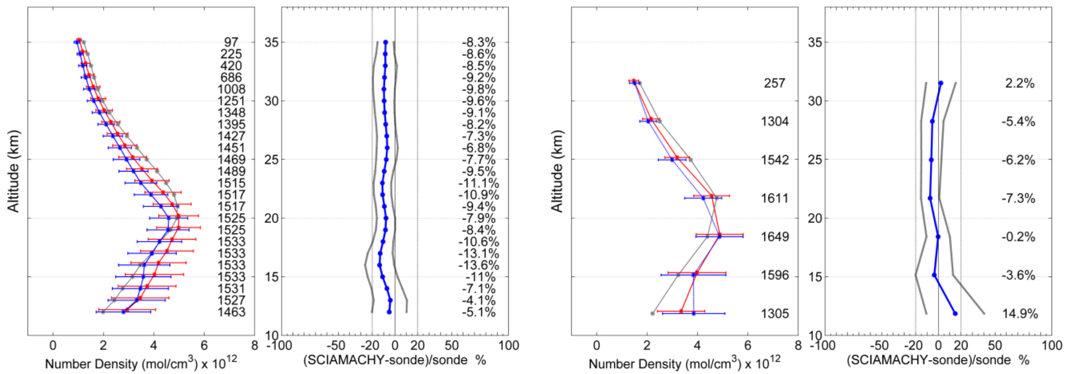

Figure 5. Same as Fig. 2 but for Eureka (80.0° N, 85.9° W).

AMTD
8, 4817–4858, 2015

Title Page
Abstract | Introduction
Conclusions | References
Tables | Figures
◀I | ▶I
◀ | ▶
Back | Close
Full Screen / Esc
Printer-friendly Version
Interactive Discussion

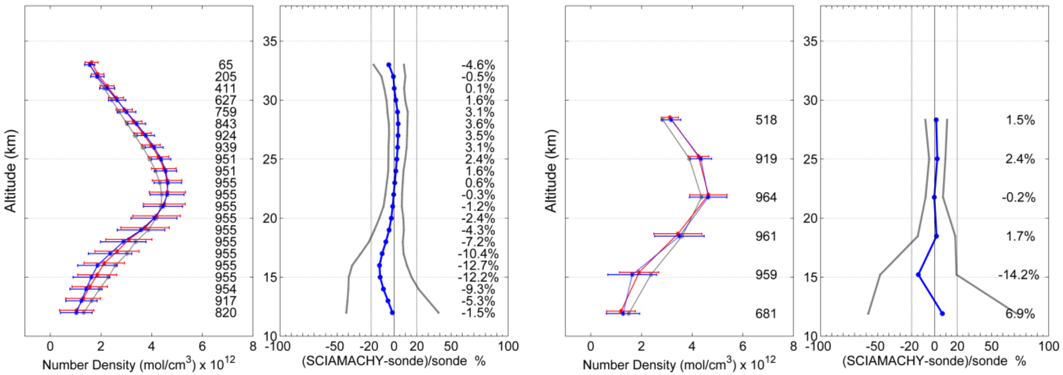

Figure 6. Same as Fig. 2 but for Lauder (44.9° S, 169.7° E).

AMTD
8, 4817–4858, 2015

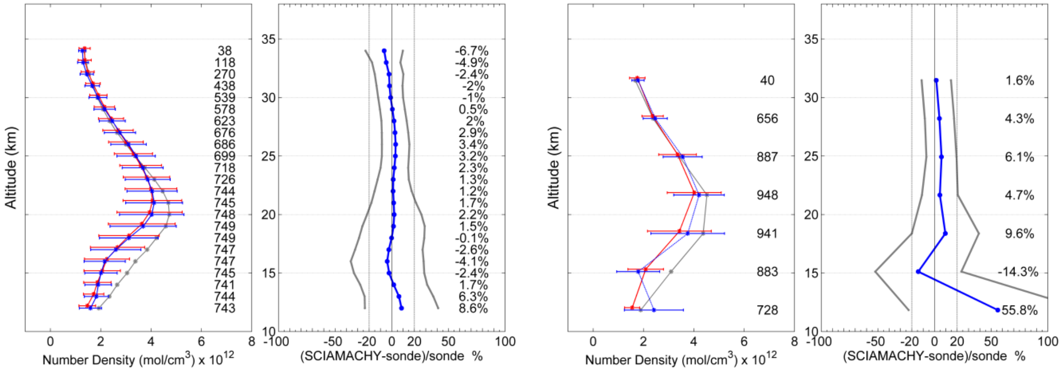

Figure 7. Same as Fig. 2 but for Marambio (64.2° S, 56.6° W).

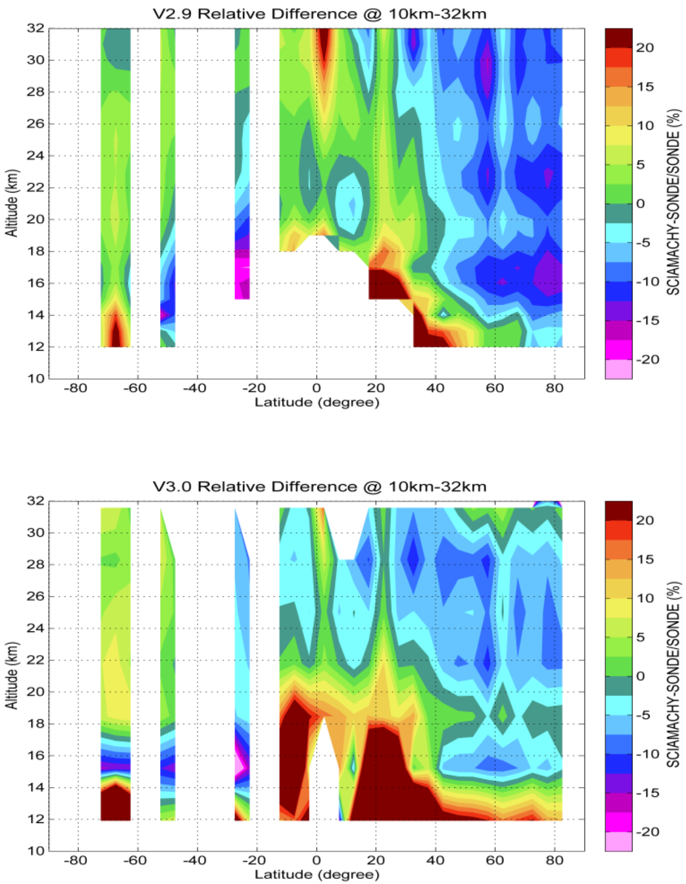

Figure 8. The altitude vs. latitude cross section of the relative differences. V2.9 in the upper panel and V3.0 in the lower panel. The improvement is mainly in the NH high latitudes.

AMTD
8, 4817–4858, 2015

Global validation of improved SCIAMACHY scientific ozone limb data

J. Jia et al.

Title Page
Abstract | Introduction
Conclusions | References
Tables | Figures
◂◂ | ▸▸
◂ | ▸
Back | Close
Full Screen / Esc
Printer-friendly Version
Interactive Discussion

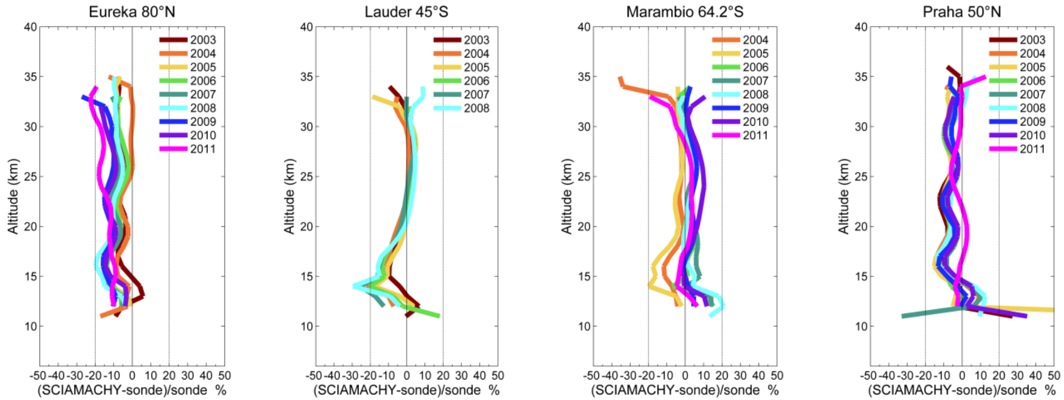

Figure 9. Yearly vertical profile comparisons of the relative differences between SCIAMACHY and ozone sondes at Eureka, Lauder, Marambio and Praha.

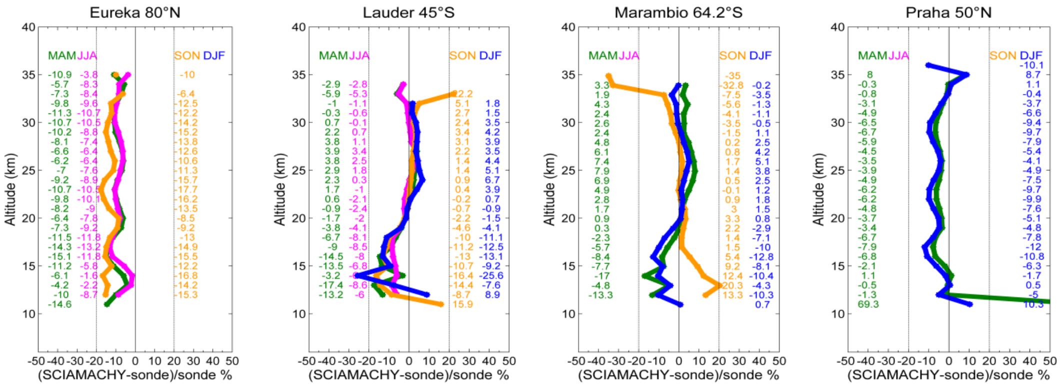

Figure 10. V2.9 seasonal vertical profile comparisons of the relative differences between SCIAMACHY and ozone sondes from 2003 to 2011 at Eureka, Lauder, Marambio and Praha. No/not enough corresponding measurements in DJF for Eureka, JJA for Marambio and in JJA and SON for Praha.

AMTD
8, 4817–4858, 2015

Global validation of improved SCIAMACHY scientific ozone limb data

J. Jia et al.

Title Page
Abstract Introduction
Conclusions References
Tables Figures
◄ ►
Back Close
Full Screen / Esc
Printer-friendly Version
Interactive Discussion

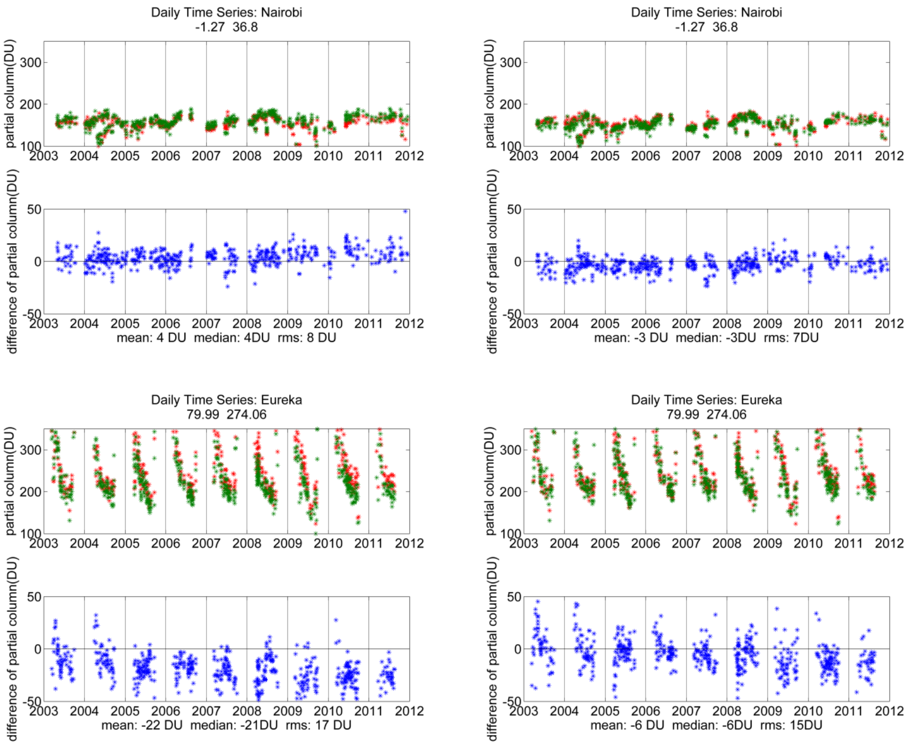

Figure 11. Time series of stratospheric ozone partial columns from SCIAMACHY V2.9/V3.0 (left/right panels) limb data (green), ozone sonde data (red) (upper panel) and their absolute difference in SCs (blue) in DU. The results are presented unsmoothed.

AMTD
8, 4817–4858, 2015

AMTD

8, 4817–4858, 2015

Global validation of improved SCIAMACHY scientific ozone limb data

J. Jia et al.

Title Page
Abstract | Introduction
Conclusions | References
Tables | Figures
◀| |▶
◀ ▶
Back | Close
Full Screen / Esc
Printer-friendly Version
Interactive Discussion

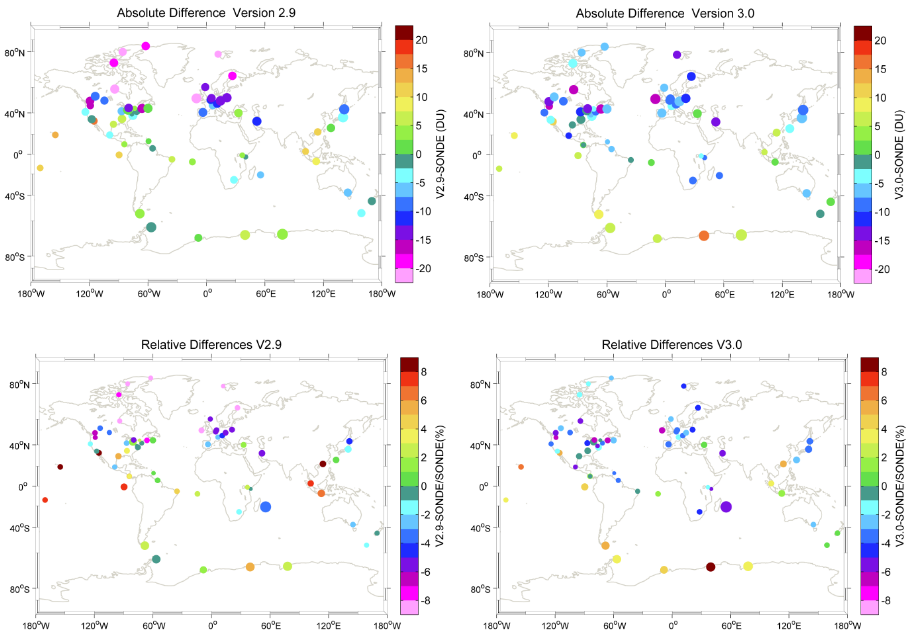

Figure 12. Comparison with all considered ozone sonde station data for the averaged daily differences in partial columns over the entire time period. The upper panels are the absolute differences; The lower panels are the relative differences. In each panel, the color of the dots depicts the mean difference/relative mean difference while the size of the dots represents 1σ SD.

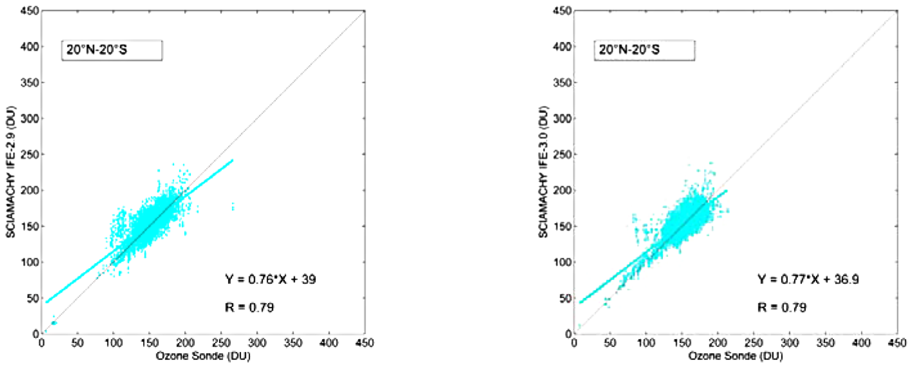

Figure 13. Scatter plots of the partial columns from SCIAMACHY and ozone sonde data within 20° S–20° N latitude bin. Left panels from V2.9; right panels from V3.0.

AMTD
8, 4817–4858, 2015

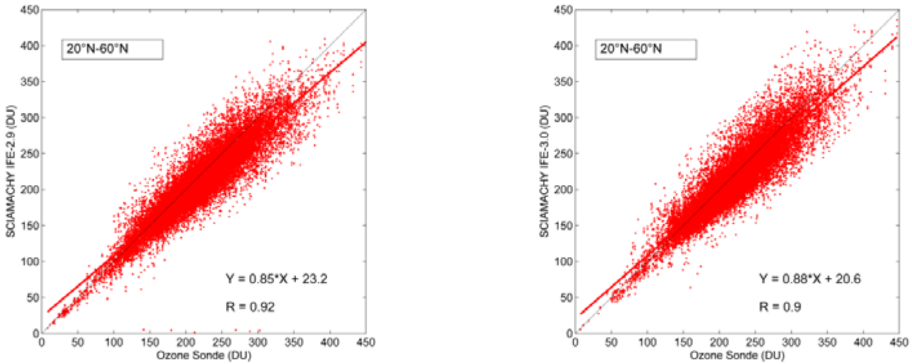

Figure 14. Same as Fig. 13 but for 20–60° N.

AMTD
8, 4817–4858, 2015

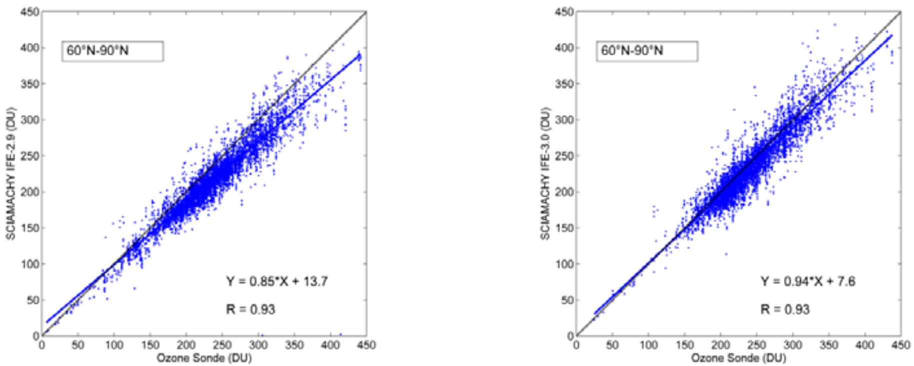

Figure 15. Same as Fig. 13 but for 60–90° N.

AMTD
8, 4817–4858, 2015

Global validation of improved SCIAMACHY scientific ozone limb data

J. Jia et al.

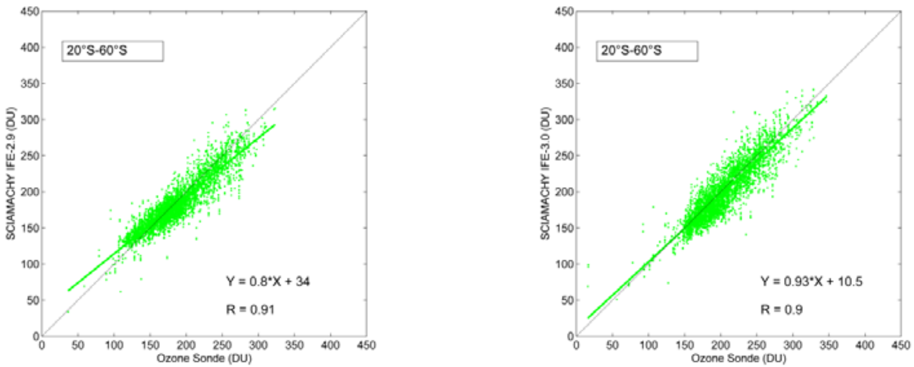

Figure 16. Same as Fig. 13 but for 20–60° S.

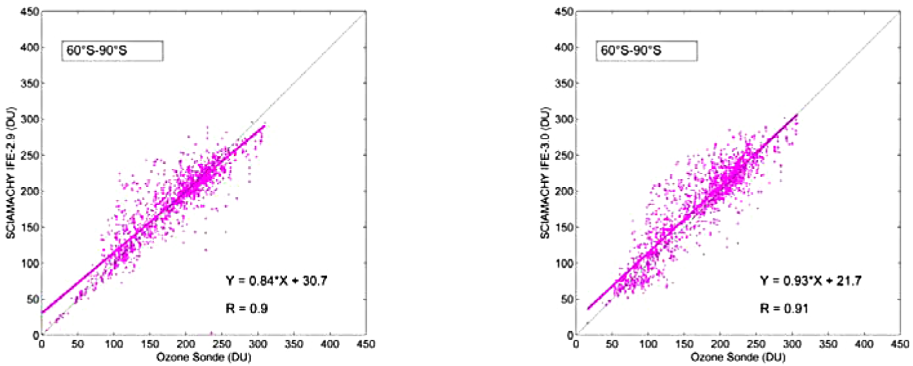

Figure 17. Same as Fig. 13 but for 60–90° S.

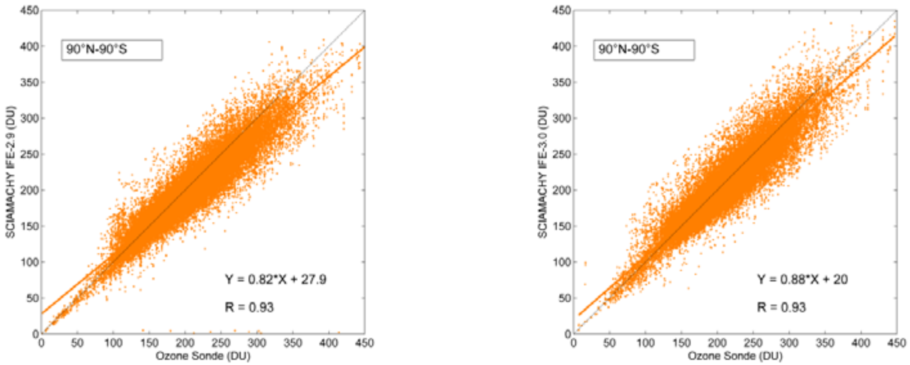

Figure 18. Same as Fig. 13 but for 90° S–90° N.

AMTD
8, 4817–4858, 2015

Global validation of improved SCIAMACHY scientific ozone limb data

J. Jia et al.

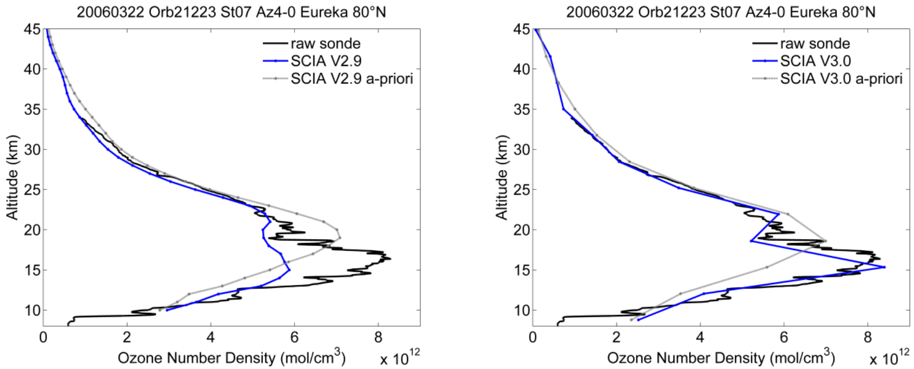

Figure 19. Comparison of ozone vertical profiles from SCIAMACHY and from ozone sonde at station Eureka.

AMTD
8, 4817–4858, 2015

Global validation of improved SCIAMACHY scientific ozone limb data

J. Jia et al.

Title Page
Abstract | Introduction
Conclusions | References
Tables | Figures
◂ ▸
Back | Close
Full Screen / Esc
Printer-friendly Version
Interactive Discussion